Available online at www.sciencedirect.com
ScienceDirect
Journal of Computational Physics 227 (2007) 537–556
JOURNAL OF COMPUTATIONAL PHYSICS
www.elsevier.com/locate/jcp

A perfectly matched layer approach to the nonlinear Schrödinger wave equations

Chunxiong Zheng

Department of Mathematical Sciences, Tsinghua University, Beijing 100084, PR China

Received 10 August 2006; received in revised form 31 July 2007; accepted 2 August 2007
Available online 16 August 2007

Abstract

Absorbing boundary conditions (ABCs) are generally required for simulating waves in unbounded domains. As one of those approaches for designing ABCs, perfectly matched layer (PML) has achieved great success for both linear and nonlinear wave equations. In this paper we apply PML to the nonlinear Schrödinger wave equations. The idea involved is stimulated by the good performance of PML for the linear Schrödinger equation with constant potentials, together with the time-transverse invariant property held by the nonlinear Schrödinger wave equations. Numerical tests demonstrate the effectiveness of our PML approach for both nonlinear Schrödinger equations and some Schrödinger-coupled systems in each spatial dimension.

Keywords: Absorbing boundary condition; Perfectly matched layer; Nonlinear Schrödinger equation; Schrödinger–Poisson system

1. Introduction

Wave problems in unbounded domains exist in many fields of application, such as quantum mechanics, optics, acoustics, geophysics, electromagnetics and aerodynamics [24]. For many such instances, the aim of numerical simulation is to compute the wave function around a small bounded part of domain which bears special physical interest. A common practice of accomplishing this is to limit the computational domain and solve a "truncated" problem with a suitable domain-based method, such as finite element or finite difference. The computational domain is usually tailored as small as possible, but at least it should contain the physically interested part. To make complete the truncated problem, special boundary conditions should be designed and applied at the domain boundary. In principle, these boundary conditions should mimic the absorption of waves into the unbounded exterior, and right in this sense, they are usually referred to as absorbing boundary conditions (ABCs) in the literature. Other names of same spirit are also popularly used, such as non-reflecting boundary conditions, transmitting boundary conditions and transparent boundary conditions.

E-mail address: czheng@math.tsinghua.edu.cn

0021-9991/$ - see front matter © 2007 Elsevier Inc. All rights reserved.
doi:10.1016/j.jcp.2007.08.004

In terms of the taxonomy of Guddati and Lim [26], most of the existing ABCs for wave problems can be classified into two categories: PDE-based and material-based. PDE-based ABCs are applied at prescribed artificial boundaries, and obtained either by factorizing the field equation and allowing only outgoing waves, or by solving the exterior wave problems with an analytical or semi-analytical method. In terms of the forms of formulation, PDE-based ABCs can be further classified into two sub-categories: local and global. Local ABCs are presented with a set of differential relations. They are computationally efficient, but usually contain two contradictory elements: accuracy and stability. Comparatively, global ABCs, which attempt to realize the complete absorption of waves, usually lead to well-approximated and well-posed truncated problems. However, from the implementational point of view, these ABCs are expensive for large-scale wave problems. This is typically because global ABCs are usually formulated in a pseudodifferential form, which contains convolution operations either in space or time, or both. Another great disadvantage of global ABCs is that they are difficult to derive for nonlinear problems. Up to now it is only possible for some specific nonlinear equations, see [30,53,23,54]. On the PDE-based ABCs for wave problems, Givoli [25], Tsynkov [51] and Hagstrom [27,28] are some good reviews.

Material-based ABCs employ a different philosophy. Instead of using artificial boundaries to limit the computational domain, they resort to a finite-thickness lossy material surrounding the physically interested part to annihilate the outgoing waves. These ABCs became extremely popular and successful after Bérenger proposed perfectly matched layer (PML) in 1994 for computational electromagnetics [14], and Chew et al. [16] offered a wonderful interpretation that PML was in fact equivalent to a continuation of the real coordinate into the complex plane. This interpretation together with many later developments [18,41] makes it possible to extend PML to more complicated problems. For example, Hu [34] has applied PML to the nonlinear Euler equations recently.

The designing of ABCs for the linear Schrödinger (LS) equation dates back to the early 1980's in [40], where the exact ABC was presented by Papadakis for the one-dimensional (1D) LS equation in underwater acoustics. Later, it was rederived independently by many authors from different application fields [8,13,31]. This exact ABC is global in time and involves a temporal half-order derivative operator. Discretization of this half-order derivative operator turns out to be a delicate issue, since any unsuitable choice, as Mayfield [39] pointed out, may destroy the underlying stability of the interior Crank–Nicolson scheme and lead to an ill-posed problem. Many authors have worked on remedying this problem. For example, instead of discretizing the exact continuous ABC for the 1D LS equation, Schmidt et al. [20,22,45], Antoine and Besse [3] derived the exact ABC for the semi-discretized equation in time. The advantage of this treatment lies in the fact that the unconditional stability of the Crank–Nicolson scheme can be maintained automatically. Arnold and Ehrhardt [8] used a different strategy. They first performed discretization in both time and space, and then derived an exact completely-discrete ABC. Again, the stability of the Crank–Nicolson scheme is preserved. Besides, their numerical experiments showed the accuracy of numerical solutions could be greatly improved. Sun and Wu [48] proposed another idea. Instead of changing discretization of the exact continuous ABC in [13], they modified the interior discretization scheme. A special finite difference scheme was designed, and shown to be unconditionally stable in concert with the discretization in [13].

For the two-dimensional (2D) LS equation, Schädle [44] presented an exact ABC in a form of integral equation and designed a numerical scheme. Han and Huang [29] derived an exact ABC in a series form at a circular artificial boundary. Arnold, Ehrhardt and Sofronov [9] studied the completely-discrete exact ABC for the LS equation in waveguides. The above work is concerned with global ABCs. Local ABCs have also been studied. For example, Antoine, Besse and Mouysset [5], Szeftel [50] designed local ABCs for the 2D LS equation at arbitrary curved artificial boundary with the pseudodifferential operator theory. Fevens and Jiang [21] extended Higdon's idea [32,33] of designing high-order local ABCs to the LS equation in any dimension. The fast evaluation of global ABCs can be also classified into the category of local ABCs. On this subject, Arnold, Ehrhardt and Sofronov [9], Jiang and Greengard [35], Lubich and Schädle [37], and Alonso-Mallo and Reguera [2] have made great contributions.

During the last several years, increasing attention has been attracted on ABCs for the nonlinear Schrödinger (NLS) equation. The first result on this subject, to the author's knowledge, is given by Fokas [23]. By the inverse scattering theory, Fokas presented an exact ABC for the 1D cubic NLS equation. Since a double integral gets involved which makes it unsuitable for numerical purposes, Zheng [54] modified Fokas' ABC and

designed a numerical scheme. By the tool of pseudodifferential operators, Antoine, Besse and Descombes [4] constructed a series of integro-differential ABCs for the same equation. Relying on the pseudodifferential calculus and paradifferential calculus, Szeftel [49] derived two families of ABCs for a general 1D NLS equation. Very recently, Soffer and Stucchio [46] presented a new algorithm of solving a general semilinear Schrödinger equation. The idea involved is to solve the semilinear Schrödinger equation on a box with periodic boundary conditions, and decompose the solution into a family of coherent states. The absorption of waves is then realized by deleting those outgoing coherent states.

In comparison to the great deal of work on PDE-based ABCs, the work on material-based ABCs for the LS and NLS equations is rather little [17,28]. In this paper, we intend to apply PML to the nonlinear Schrödinger wave equations. The idea is stimulated by the good performance of PML for the 1D LS equation with constant potentials, and the time-transverse invariant property of the nonlinear Schrödinger wave equations. Its effectiveness will be demonstrated through numerical tests under different settings of problem.

The rest of this paper is as follows. In Section 2, we explain the PML idea for the LS equation with constant potentials, and in Section 3, we extend it for the LS equation with variable potentials. In Section 4, the PML is applied to the 1D NLS equation, and a time-splitting central difference scheme is proposed. Application of PML for the high-dimensional NLS equation is considered in Section 5. The alternating direction implicit (ADI) scheme is used to overcome the difficulty arising from high dimensions. In Section 6, the PML technique is further extended for the Schrödinger-coupled systems. A time-splitting fast sine transformation (FST) scheme is presented for the model Schrödinger-Poisson system in waveguide. This paper concludes in Section 7.

2. 1D LS equation with constant potentials

We start with the 1D LS equation with a constant potential $V \in \mathbf{R}$

$$\mathrm{i}\partial_t u + \partial_x^2 u = Vu. \tag{2.1}$$

The initial function $u_0(x)$ is supposed to be compactly supported in a finite interval $[x_L, x_R]$. In this context, Eq. (2.1) models wave propagation from $[x_L, x_R]$ to $(-\infty, x_L]$ and $[x_R, +\infty)$ through two boundary points $\{x_L, x_R\}$. To compute the wave function u in $[x_L, x_R]$, two ABCs are required at the boundary points $\{x_L, x_R\}$. We can derive them with modal analysis on the two semi-infinite intervals $(-\infty, x_L]$ and $[x_R, +\infty)$, as explained in the following.

We first consider Eq. (2.1) restricted to $[x_R, +\infty)$. Let the modal solution be

$$u = \mathrm{e}^{\lambda x + st}, \tag{2.2}$$

where s with $\Re s > 0$ is the argument in the Laplace-transformed space. Substituting (2.2) into (2.1) we get immediately

$$\mathrm{i}s + \lambda^2 = V.$$

Since wave travels out of $[x_L, x_R]$, the energy of each modal solution should be finite, which implies

$$\lambda = -\sqrt{-\mathrm{i}s + V}.$$

It is easy to verify that if s runs around the right half complex plane, λ will run around the second quadrant. See left and middle plots of Fig. 1. Each λ-curve corresponds to a straight s-curve. Note that for any fixed s-curve, changing V will not change the corresponding λ-curve, but the point location only.

The PML technique can be taken as a coordinate stretching from real space to complex plane. More precisely, let R be a complex number, and we make the following coordinate transformation

$$x' = x + R\int_{x_R}^{x} \sigma(r)\mathrm{d}r.$$

Here σ, referred to as the *absorption function* later, is continuous and nonnegative which vanishes outside of $[x_R, +\infty)$. The modal solution (2.2) is modified accordingly to

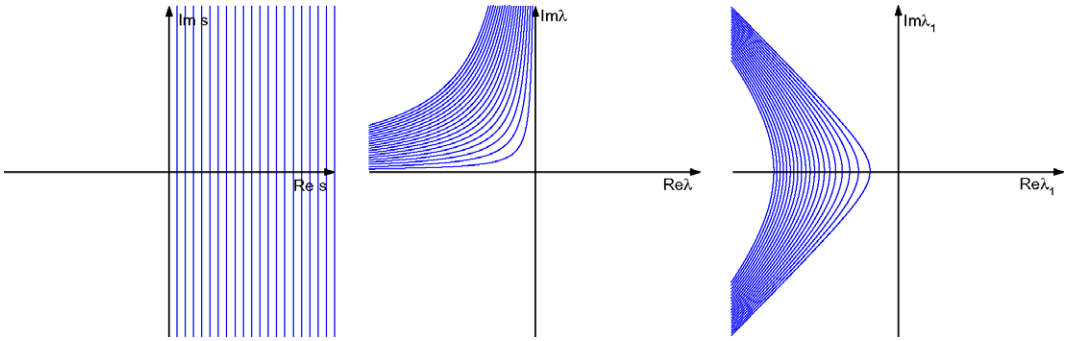

Fig. 1. Variable transformations. Left: s. Middle: $\lambda = -\sqrt{-is + V}$. Right: $\lambda_1 = \lambda e^{i\pi/4}$.

$$u' = e^{\lambda x' + st}. \tag{2.3}$$

Note that in $(-\infty, x_R]$ we have $x' = x$, and thus $u' = u$. Since

$$\frac{\partial x'}{\partial x} = 1 + R\sigma,$$

all the modified modal solution u' satisfies

$$i\partial_t u + \frac{1}{1+R\sigma}\partial_x\left(\frac{1}{1+R\sigma}\partial_x u\right) = Vu. \tag{2.4}$$

This equation coincides with the LS equation (2.1) on $(-\infty, x_R]$, but differs on $[x_R, +\infty)$. Since

$$u' = e^{\lambda\left(x+R\int_{x_R}^{x}\sigma(r)dr\right)+st} = e^{\lambda x+st}\cdot e^{\lambda R\int_{x_R}^{x}\sigma(r)dr} = u\cdot f, \quad \lambda_1 = \lambda R, \quad f = e^{\lambda_1\int_{x_R}^{x}\sigma(r)dr},$$

each modal solution u is modulated with a factor f (different for different s). If we choose R such that $\Re\lambda_1 < 0$, then u' decays exponentially faster than u as x goes to $+\infty$. This implies that in principle the solution of Eq. (2.4) damps faster in $[x_R, +\infty)$ than the solution of the original LS equation (2.1) does. If this damping is fast enough, it is justified in truncating the semi-infinite interval $[x_R, +\infty)$ into a finite one, say $[x_R, x_{RP}]$, and impose zero *Dirichlet boundary condition* (DBC) at the boundary point x_{RP}. Therefore, being restricted to $(-\infty, x_R]$, the solution of Eq. (2.4) expects to be a reasonable approximation to the solution of Eq. (2.1). The accuracy depends on the amplitude of f at x_{RP}, i.e.

$$|f(x_{RP})| = e^{\Re\lambda_1\int_{x_R}^{x_{RP}}\sigma(r)dr}.$$

The bigger the quantity $\int_{x_R}^{x_{RP}}\sigma(r)dr$ is, the more accurate the approximation becomes since we have already assumed $\Re\lambda_1 < 0$.

The left semi-infinite interval $(-\infty, x_L]$ can be handled analogously. We carefully choose the absorption function σ in an interval, say $[x_{LP}, x_L]$, and impose zero DBC at x_{LP}. Combining the results for both semi-infinite intervals, we derive an equation defined only in the finite interval $[x_{LP}, x_{RP}]$

$$i\partial_t u + c\partial_x(c\partial_x u) = Vu, \tag{2.5}$$

with $c = 1/(1 + R\sigma)$. This equation will be referred to as the PML equation in the following.

We need to determine the complex number R and the absorption function σ. The choice of R is rather optional. Note that λ lies in the second quadrant, see Fig. 1. To ensure a negative real part of $\lambda_1 = \lambda R$, R can be any complex number in the first quadrant. The optimal choice relies of course on the energy distribution of modal solutions. Since this issue is problem-dependent, we set $R = e^{i\pi/4}$ thus $\lambda_1 = \lambda e^{i\pi/4}$ for an average effect. See the right plot of Fig. 1.

There are two choices for the absorption function σ. The first one is classical [14,18]. It uses low-degree power functions. The second one is a new development by Bermúdez et al. [15]. They used singular functions. In this paper we let σ be quadratic function in the absorbing layers, i.e.

$$\sigma = \begin{cases} \sigma_0(x - x_{\mathrm{L}})^2, & x_{\mathrm{LP}} < x < x_{\mathrm{L}}, \\ 0, & x_{\mathrm{L}} < x < x_{\mathrm{R}}, \\ \sigma_0(x - x_{\mathrm{R}})^2, & x_{\mathrm{R}} < x < x_{\mathrm{RP}}, \end{cases} \tag{2.6}$$

where $\sigma_0 > 0$ is referred to as the *absorption strength factor*. In this case, the absorbing effect of PML only depends on two parameters: the absorption strength factor and the thickness of absorbing layer. Take the right absorbing layer $[x_{\mathrm{R}}, x_{\mathrm{RP}}]$ as an example. Since

$$\int_{x_{\mathrm{R}}}^{x_{\mathrm{RP}}} \sigma(r)\mathrm{d}r = \frac{\sigma_0(x_{\mathrm{RP}} - x_{\mathrm{R}})^3}{3}, \tag{2.7}$$

we expect that the thickness of absorbing layer $D \equiv x_{\mathrm{RP}} - x_{\mathrm{R}}$ has more significant effect than the absorption strength factor.

The PML equation (2.5) is then solved with a numerical scheme in the interval $[x_{\mathrm{LP}}, x_{\mathrm{RP}}]$. For an easy generalization to high-dimensional problems, we employ the Crank–Nicolson central difference scheme in this paper. Let M be a positive integer, $h = (x_{\mathrm{RP}} - x_{\mathrm{LP}})/M$ the spatial stepsize, and Δt the time step. Besides, we let

$$t_n = n\Delta t, \quad x_k = x_{\mathrm{LP}} + kh, \quad c_k = c(x_k), \quad U_k^n \sim u(x_k, t_n),$$

$$\widetilde{D}_x^2 U_k^n = \frac{c_k c_{k-\frac{1}{2}}}{h^2} U_{k-1}^n - \frac{c_k\left(c_{k-\frac{1}{2}} + c_{k+\frac{1}{2}}\right)}{h^2} U_k^n + \frac{c_k c_{k+\frac{1}{2}}}{h^2} U_{k+1}^n.$$

Our scheme reads

$$U_k^0 = u_0(x_k), \quad U_0^n = U_M^n = 0, \tag{2.8}$$

$$\frac{2\mathrm{i}}{\Delta t} U_k^{n+1} + \widetilde{D}_x^2 U_k^{n+1} - VU_k^{n+1} = \frac{2\mathrm{i}}{\Delta t} U_k^n - \widetilde{D}_x^2 U_k^n + VU_k^n \tag{2.9}$$

with $k = 1, \ldots, M-1$ and $n = 0, 1, \ldots$. At each time step, we need solve a linear algebraic system with an M-by-M tridiagonal coefficient matrix, which can be accomplished efficiently within $\mathrm{O}(M)$ operations.

The LS equation (2.1) admits an exact solution

$$u_{\mathrm{exa}} = \sqrt{\frac{\mathrm{i}}{-4t + \mathrm{i}}} \exp\left(\frac{-\mathrm{i}x^2 - k_0 x + k_0^2 t}{-4t + \mathrm{i}} - \mathrm{i}Vt\right),$$

which represents a traveling Gaussian beam with velocity $2k_0$ (the width increases). It has been used as numerical example in [3] with $V = 0$ and $k_0 = 8$. At the initial time we have

$$u_0(x) = \exp(-x^2 + \mathrm{i}k_0 x), \tag{2.10}$$

which is close to zero with an error less than 1.3888×10^{-11} outside of $[-5, 5]$. This justifies us in setting the physical domain as $[x_{\mathrm{L}}, x_{\mathrm{R}}] = [-5, 5]$. To evaluate the approximating accuracy of the PML equation, we define the *normalized* L^2-error as

$$\frac{||u_{\mathrm{pml}} - u_{\mathrm{exa}}||_{0,[x_{\mathrm{L}},x_{\mathrm{R}}]}}{||u_0||_{0,[x_{\mathrm{L}},x_{\mathrm{R}}]}},$$

where u_{pml} is the solution to the PML equation. Since u_{pml} is generally unknown, we compute it by scheme (2.8)–(2.9) with $\Delta t = 0.00001$ and $h = 0.0001$, which are small enough to neglect discretization error. These parameters are also used in the numerical examples of next two sections.

In the left plot of Fig. 2, we depict errors for different absorption strength factors. The thickness of absorbing layers is $D = 0.5$, i.e. $[x_{\mathrm{LP}}, x_{\mathrm{RP}}] = [-5.5, 5.5]$. For ease of reference, we use the magenta curve (the thin one joining A and B_1) to show the *normalized* L^2-norm of u_{exa} defined by

$$\frac{||u_{\mathrm{exa}}||_{0,[x_{\mathrm{L}},x_{\mathrm{R}}]}}{||u_0||_{0,[x_{\mathrm{L}},x_{\mathrm{R}}]}}.$$

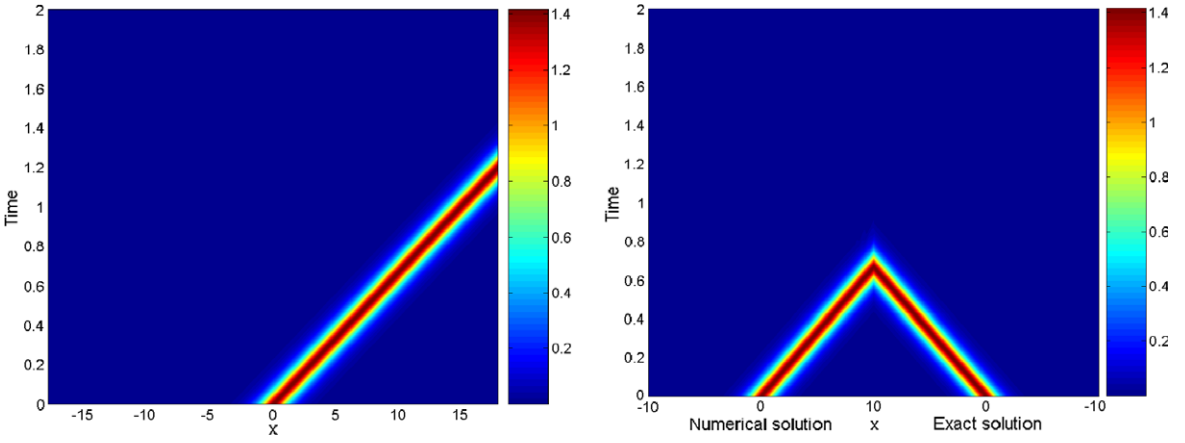

Fig. 7. Cubic NLS equation with $V = -2|u|^2$. Left: Exact solution. Right: Comparison. The numerical solution is computed with $D = 1$ and $\sigma_0 = 5$.

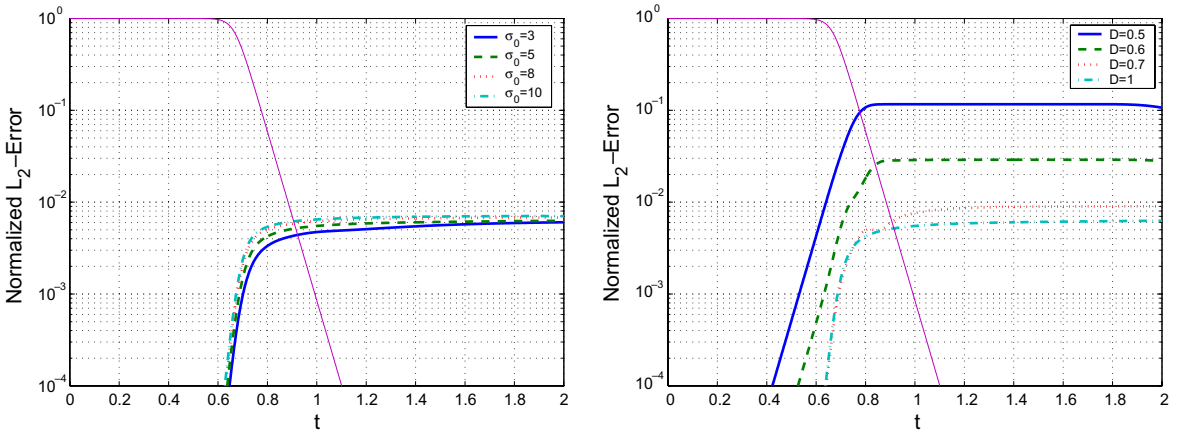

Fig. 8. Cubic NLS equation with $V = -2|u|^2$. Left: $D = 1$. Right: $\sigma_0 = 5$.

A direct computation shows

$$E(u_0) \approx 80.5478 > 0,$$

which implies the blow-up will not occur for this numerical test. We depict the exact solution in the left plot of Fig. 9, and make comparison between the numerical solution and the exact solution in the right plot. Numerical errors are shown in Fig. 10. Similar observations as those for the cubic numerical test case can be made.

In the real applications, especially for high-dimensional problems, the grid parameters cannot be chosen as small as those used in the above numerical tests. This means besides the approximate PML ABC, the spatial-temporal discretization can be another significant source of error. Let us go back to the numerical test on the cubic NLS equation. In Fig. 11, we depict the errors between the numerical solutions and the exact solutions for different spatial and time steps. At the initial stage (before $t = 0.6$), the PML layers do not take into effect since the waves have not reached the boundary points yet. The discretization error dominates, and it can be reduced by decreasing Δt and h. After $t = 0.6$, there is a transition period when waves travel through the boundary points. This period is quite short. In fact, at $t = 0.8$, only 6% of the total energy is left in the physical domain $[x_L, x_R]$. During the time period [0.6, 0.8], the error from PML layers becomes more and more significant, and the effect of decreasing Δt and h becomes more and more limited. After $t = 0.8$, the error from PML layers completely dominates, while the influence of spatial-temporal discretization becomes less important.

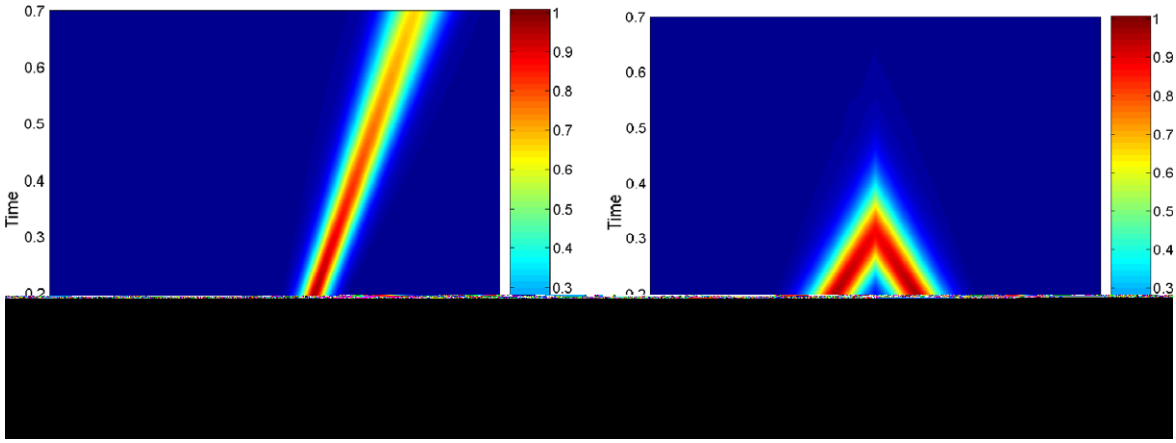

Fig. 9. Quintic NLS equation with $V = -2|u|^4$. Left: Exact solution. Right: Comparison. The numerical solution is computed with $D = 1$ and $\sigma_0 = 5$.

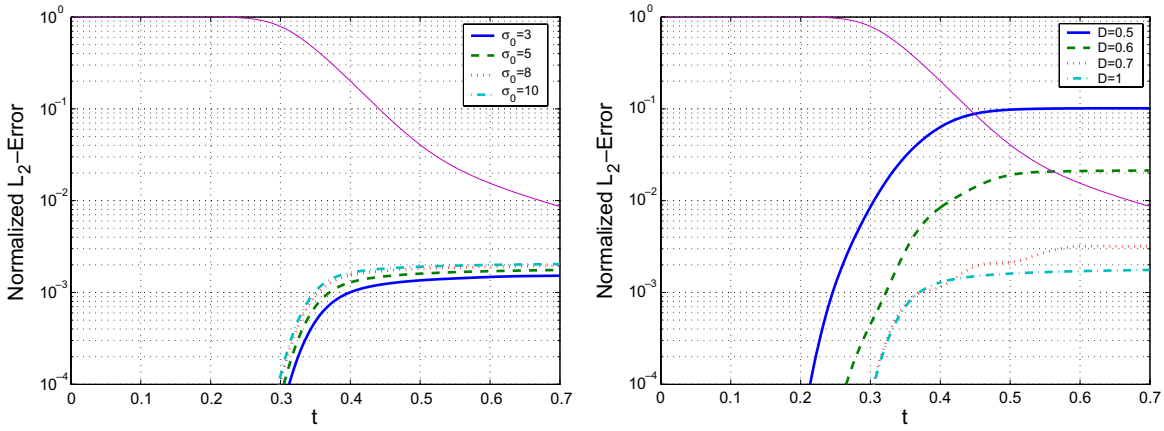

Fig. 10. Quintic NLS equation with $V = -2|u|^4$. Left: $D = 1$. Right: $\sigma_0 = 5$.

5. High-dimensional NLS equation

A remarkable advantage of PML for the Schrödinger wave equations lies in the easy extension to high dimensions. In this section we will show how this can be done. For simplicity and brevity, we confine ourselves to the NLS equation in two dimensions

$$\mathrm{i}\partial_t u + \partial_x^2 u + \partial_y^2 u = V(x, y, t, |u|^2)u. \tag{5.1}$$

The initial function is supposed to be compactly supported in a rectangular domain $[x_L, x_R] \times [y_L, y_R]$. We simply modify the (5.1) with the PML technique in x- and y-directions independently, and obtain an equation on an enlarged domain $[x_{LP}, x_{RP}] \times [y_{LP}, y_{RP}]$

$$\mathrm{i}\partial_t u + c_1\partial_x(c_1\partial_x u) + c_2\partial_y(c_2\partial_y u) = V(x, y, t, |u|^2)u. \tag{5.2}$$

Here, $c_1 = 1/(1 + R\sigma_1)$ and $c_2 = 1/(1 + R\sigma_2)$ with

$$\sigma_1(x) = \begin{cases} \sigma_0(x - x_L)^2, & x_{LP} < x < x_L, \\ 0, & x_L < x < x_R, \\ \sigma_0(x - x_R)^2, & x_R < x < x_{RP}. \end{cases}, \quad \sigma_2(y) = \begin{cases} \sigma_0(y - y_L)^2, & y_{LP} < y < y_L, \\ 0, & y_L < y < y_R, \\ \sigma_0(y - y_R)^2, & y_R < y < y_{RP}. \end{cases}$$

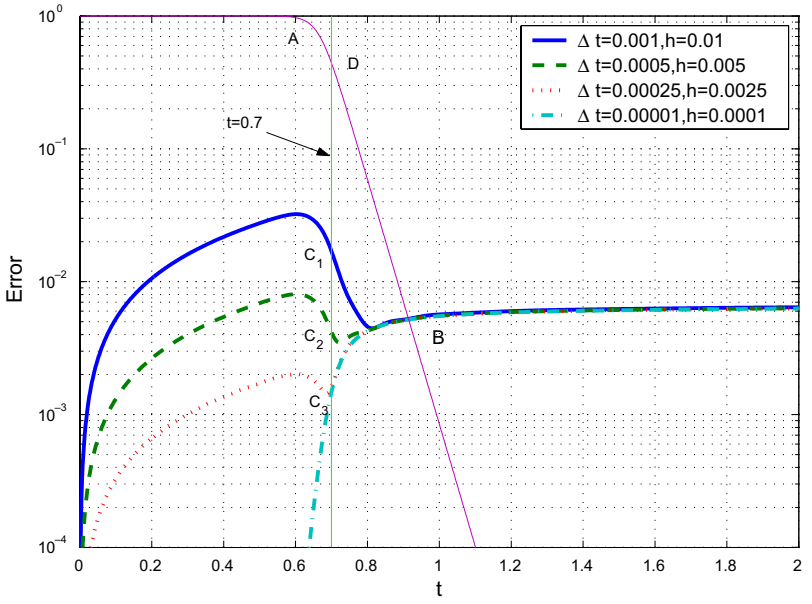

Fig. 11. Cubic NLS equation with $V=-2|u|^2$. $D=1$ and $\sigma_0=5$.

Again, zero DBC is imposed at the boundary of $[x_{\mathrm{LP}},x_{\mathrm{RP}}]\times[y_{\mathrm{LP}},\ y_{\mathrm{RP}}]$.

For the constant potential LS equation in two dimensions, the PML Eq. (5.2) results perfect matching to the interior governing equation. Since dissipation is supplemented in both two directions, the solution of (5.2) is also fast damping and long-time stable. These points fully justify the applicability of the PML for high-dimensional Schrödinger wave equations. We would remark that this merit of the PML is not universal at all. For most hyperbolic systems, it is still an open issue to design a high-dimensional PML formulation which is perfect matching, fast damping and long-time stable, see [6]. But for the Maxwell's equations, this issue is largely solved, see [10].

Now let us consider the semi-discretization in time. Set $u^n(x,y)\sim u(x,y,t_n)$. Again, the time-splitting technique is employed to handle the nonlinearity in (5.2). Given u^n, we compute u^{n+1} with two steps. First, we solve the nonlinear equation

$$\mathrm{i}\partial_t u = V(x,y,t,|u|^2)u, \tag{5.3}$$

with the initial data u^n in $[t_n,t_{n+1}]$, to obtain $u^*=u(t_{n+1})$. Then, we solve the linear equation

$$\mathrm{i}\partial_t u + c_1\partial_x(c_1\partial_x u) + c_2\partial_y(c_2\partial_y u) = 0, \tag{5.4}$$

with the initial data u^* in $[t_n,t_{n+1}]$ again, to obtain u^{n+1}.

Next we consider spatial discretization. Let

$$h_x=\frac{x_{\mathrm{RP}}-x_{\mathrm{LP}}}{M},\quad h_y=\frac{y_{\mathrm{RP}}-y_{\mathrm{LP}}}{N},\quad x_k=x_{\mathrm{LP}}+kh_x,\quad y_l=y_{\mathrm{LP}}+lh_y, \tag{5.5}$$

$$c_{1,k}=c_1(x_k),\quad c_{2,l}=c_2(y_l),\quad U^n_{k,l}\sim u(x_k,y_l,t_n), \tag{5.6}$$

$$\widetilde{D}_x^2U^n_{k,l}=\frac{c_{1,k}c_{1,k-\frac12}}{h_x^2}U^n_{k-1,l}-\frac{c_{1,k}\left(c_{1,k-\frac12}+c_{1,k+\frac12}\right)}{h_x^2}U^n_{k,l}+\frac{c_{1,k}c_{1,k+\frac12}}{h_x^2}U^n_{k+1,l}, \tag{5.7}$$

$$\widetilde{D}_y^2U^n_{k,l}=\frac{c_{2,l}c_{2,l-\frac12}}{h_y^2}U^n_{k,l-1}-\frac{c_{2,l}\left(c_{2,l-\frac12}+c_{2,l+\frac12}\right)}{h_y^2}U^n_{k,l}+\frac{c_{2,l}c_{2,l+\frac12}}{h_y^2}U^n_{k,l+1}. \tag{5.8}$$

Analogous to the analysis of Eqs. (4.5) and (5.3) is solved by

$$U^*_{k,l} = U^n_{k,l} e^{-\frac{i\Delta t}{2}\left(V\left(x_k,y_l,t_n,|U^n_{k,l}|^2\right)+V\left(x_k,y_l,t_{n+1},|U^n_{k,l}|^2\right)\right)}.$$

As to Eq. (5.4), a direct implementation of the Crank–Nicolson central difference scheme would lead to the following linear system

$$\frac{2i}{\Delta t}U^{n+1}_{k,l} + \widetilde{D}^2_x U^{n+1}_{k,l} + \widetilde{D}^2_y U^{n+1}_{k,l} = \frac{2i}{\Delta t}U^*_{k,l} - \widetilde{D}^2_x U^*_{k,l} - \widetilde{D}^2_y U^*_{k,l}. \tag{5.9}$$

Though the coefficient matrix is sparse, it has a large bandwidth, thus any direct solver for this linear system would be very expensive. Alternatively, on a rectangular domain with the zero DBC, an equation like (5.4) can be efficiently solved with the ADI method. Namely, Eq. (5.4) is solved with the following two steps

$$\frac{2i}{\Delta t}U^{**}_{k,l} + \widetilde{D}^2_x U^{**}_{k,l} = \frac{2i}{\Delta t}U^*_{k,l} - \widetilde{D}^2_y U^*_{k,l}, \tag{5.10}$$

$$\frac{2i}{\Delta t}U^{n+1}_{k,l} + \widetilde{D}^2_y U^{n+1}_{k,l} = \frac{2i}{\Delta t}U^{**}_{k,l} - \widetilde{D}^2_x U^{**}_{k,l}. \tag{5.11}$$

At each step, a set of linear systems with tridiagonal coefficient matrix need to be solved, which can be accomplished efficiently with the Thomas method.

Now combining the Strang's splitting technique, we derive a numerical scheme which is second order in both time and space:

Step 0: Given $U^n_{k,l}$;

Step 1: Let

$$U^*_{k,l} = U^n_{k,l} e^{-\frac{i\Delta t}{4}\left(V\left(x_k,y_l,t_n,|U^n_{k,l}|^2\right)+V\left(x_k,y_l,t_{n+1},|U^n_{k,l}|^2\right)\right)};$$

Step 2: Solve $U^{**}_{k,l}$ by

$$\frac{2i}{\Delta t}U^{**}_{k,l} + \widetilde{D}^2_x U^{**}_{k,l} = \frac{2i}{\Delta t}U^*_{k,l} - \widetilde{D}^2_y U^*_{k,l};$$

Step 3: Solve $U^{***}_{k,l}$ by

$$\frac{2i}{\Delta t}U^{***}_{k,l} + \widetilde{D}^2_y U^{***}_{k,l} = \frac{2i}{\Delta t}U^{**}_{k,l} - \widetilde{D}^2_x U^{**}_{k,l};$$

Step 4: Finally, we set

$$U^{n+1}_{k,l} = U^{***}_{k,l} e^{-\frac{i\Delta t}{4}\left(V\left(x_k,y_l,t_n,|U^{***}_{k,l}|^2\right)+V\left(x_k,y_l,t_{n+1},|U^{***}_{k,l}|^2\right)\right)}.$$

We use this scheme to study the evolution of four 2D Gaussian beams with a focusing cubic nonlinearity, i.e. we set

$$u_0(x,y) = \sum_{j=1}^{4} \exp(-x^2 - y^2 + ik_{x,j}x + ik_{y,j}y), V = -2|u|^2,$$

where $(k_{x,1},k_{y,1}) = (1,1)$, $(k_{x,2},k_{y,2}) = (-1,1)$, $(k_{x,3},k_{y,3}) = (-1,-1)$ and $(k_{x,4},k_{y,4}) = (1,-1)$. The physical domain is set to be $[x_L, x_R]\times[y_L, y_R] = [-4, 4]^2$, and the computational domain is set to be $[x_{LP}, x_{RP}]\times[y_{LP}, y_{RP}] = [-5, 5]^2$. Besides, we set $\sigma_0 = 10$, $h_x = h_y = 0.01$ and $\Delta t = 0.001$.

The solution of the 2D cubic focusing NLS equation might blow-up if the initial state energy defined as (4.10) is less than zero. For each Gaussian beam, a direct computation shows

$$E(u_0) \approx 80.5489 > 0,$$

which suggests the blow-up will not appear. In Fig. 12 we depict the numerical solutions at several time points. No reflection can be observed at the physical boundary. We should note that different colormaps are used for different snapshots of Fig. 12.

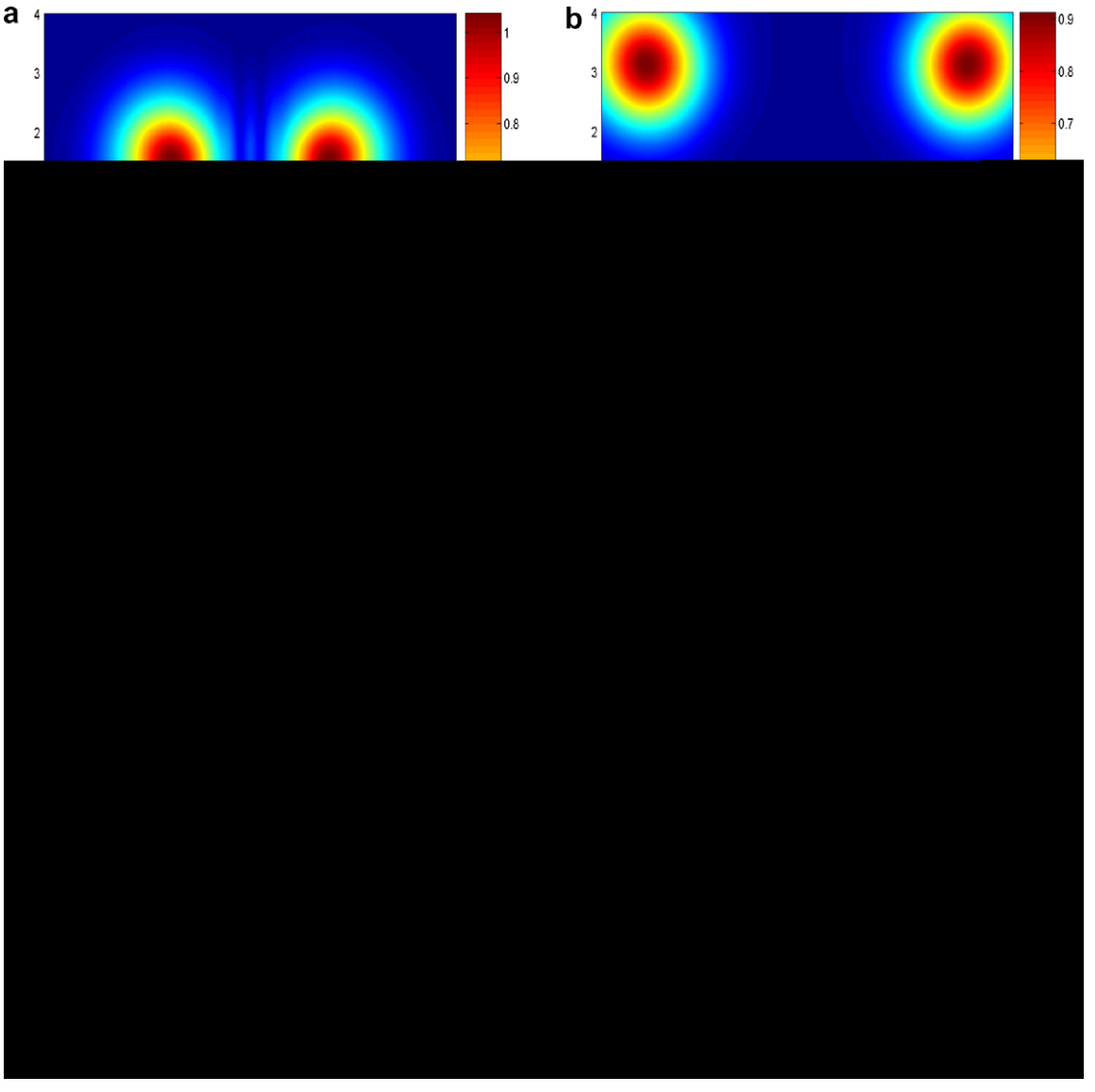

Fig. 12. Snapshots of numerical solutions for the 2D NLS equation. $V = -2|u|^2$. (a) $t = 0.1$; (b) $t = 0.2$; (c) $t = 0.3$; (d) $t = 0.4$.

6. Schrödinger-coupled systems

If the potential V of NLS equation has a global part, which means V depends on the wave function by a nonlocal means, a Schrödinger-coupled system usually brings out. There are a number of this kind of systems which play important roles in various application fields, such as plasma physics [1], molecular chains [19], and quantum transport in semi-conductor devices [7,38]. To explore the possibility of applying PML for such systems, we consider the following 2D Schrödinger-Poisson system on waveguide

$$\mathrm{i}\partial_t u + \partial_x^2 u + \partial_y^2 u = Vu, \ (x,y) \in \mathbf{R} \times [y_L, y_R], \tag{6.1}$$

$$-\partial_x^2 V - \partial_y^2 V = |u|^2, \ (x,y) \in \mathbf{R} \times [y_L, y_R]. \tag{6.2}$$

We assume the initial function u_0 is compactly supported in $[x_L, x_R] \times [y_L, y_R]$, and the zero DBC is imposed at the physical boundary for both the wave function u and the potential V. Besides, we assume u tends to zero

and V remains bounded when the location point goes to infinity. The number of studies on the well-posedness and semi-classical limit of Schrödinger-Poisson system is huge, see [36] for an example.

Applying PML on $[x_{\mathrm{LP}}, x_{\mathrm{RP}}]\times[y_{\mathrm{L}}, y_{\mathrm{R}}]$ we derive a modified Schrödinger-Poisson system

$$\mathrm{i}\partial_t u + c\partial_x(c\partial_x u) + \partial_y^2 u = Vu, (x,y) \in [x_{\mathrm{LP}}, x_{\mathrm{RP}}] \times [y_{\mathrm{L}}, y_{\mathrm{R}}], \tag{6.3}$$

$$-\partial_x^2 V - \partial_y^2 V = |u|^2, \ (x,y) \in \mathbf{R} \times [y_{\mathrm{L}}, y_{\mathrm{R}}]. \tag{6.4}$$

Now the wave function u with zero DBC is defined only on $[x_{\mathrm{LP}}, x_{\mathrm{RP}}]\times[y_{\mathrm{L}}, y_{\mathrm{R}}]$, but the potential V is still defined on the whole waveguide $\mathbf{R}\times[y_{\mathrm{L}}, y_{\mathrm{R}}]$. Notice that in Eq. (6.4), we have made a zero extension of wave function u in the outside of $[x_{\mathrm{LP}}, x_{\mathrm{RP}}]\times[y_{\mathrm{L}}, y_{\mathrm{R}}]$.

Let

$$h_y = \frac{y_{\mathrm{R}} - y_{\mathrm{L}}}{N}, \quad y_l = y_{\mathrm{L}} + lh_y, \quad u_{x,l}(t) \sim u(x, y_l, t), \quad V_{x,l}(t) \sim V(x, y_l, t), \tag{6.5}$$

$$D_y^2 u_{x,l} = \frac{1}{h_y^2} u_{x,l-1} - \frac{2}{h_y^2} u_{x,l} + \frac{1}{h_y^2} u_{x,l+1}, \quad l = 1, \ldots, N-1. \tag{6.6}$$

The semi-discretization of Eqs. (6.3)–(6.4) in y direction yields a nonlinear PDE system

$$\mathrm{i}\partial_t u_{x,l} + c\partial_x(c\partial_x u_{x,l}) + D_y^2 u_{x,l} = V_{x,l} u_{x,l}, x \in [x_{\mathrm{LP}}, x_{\mathrm{RP}}], \tag{6.7}$$

$$-\partial_x^2 V_{x,l} - D_y^2 V_{x,l} = |u_{x,l}|^2, x \in \mathbf{R}, \ l = 1, \ldots, N-1. \tag{6.8}$$

We consider the time discretization with the time-splitting technique. Let $u_{x,l}^n \sim u_{x,l}(t_n)$. Given $u_{x,l}^n$, we take two steps to derive $u_{x,l}^{n+1}$. First, we solve the nonlinear PDE system

$$\mathrm{i}\partial_t u_{x,l} = V_{x,l} u_{x,l}, \quad x \in [x_{\mathrm{LP}}, x_{\mathrm{RP}}], \tag{6.9}$$

$$-\partial_x^2 V_{x,l} - D_y^2 V_{x,l} = |u_{x,l}|^2, \quad x \in \mathbf{R}, \quad l = 1, \ldots, N-1, \tag{6.10}$$

with the initial datum $u_{x,l}^n$ in $[t_n, t_{n+1}]$, to obtain $u_{x,l}^* = u_{x,l}(t_{n+1})$. Then, we solve the linear equations

$$\mathrm{i}\partial_t u_{x,l} + c\partial_x(c\partial_x u_{x,l}) + D_y^2 u_{x,l} = 0, \quad x \in [x_{\mathrm{LP}}, x_{\mathrm{RP}}], \quad l = 1, \ldots, N-1, \tag{6.11}$$

with the initial datum $u_{x,l}^*$ in $[t_n, t_{n+1}]$ again, to obtain $u_{x,l}^{n+1} = u_{x,l}(t_{n+1})$.

From Eq. (6.9), it is direct to verify that $|u_{x,l}(t)|^2 = |u_{x,l}^n|^2$, thus Eq. (6.10) actually defines a ODE system, with the unknown functions $V_{x,l}$ coupled together. Remember that we assume the zero DBC at the physical boundary. By the fast sine transform (FST)

$$\widehat{V_{x,l'}} \overset{def}{=} 2\sum_{l=1}^{N-1} V_{x,l} \sin\frac{l' l\pi}{N}, \ \widehat{\widehat{V_{x,l}}} = 2NV_{x,l}, \tag{6.12}$$

in the transformed space, Eq. (6.10) reads

$$-\partial_x^2 \widehat{V_{x,l'}} + \lambda_{l'} \widehat{V_{x,l'}} = \widehat{|u_{x,l'}^n|^2}, \quad x \in \mathbf{R}, \quad l' = 1, \ldots, N-1, \tag{6.13}$$

where

$$\lambda_{l'} = \frac{N^2(2 - 2\cos\frac{l'\pi}{N})}{(y_{\mathrm{R}} - y_{\mathrm{L}})^2}, \quad l' = 1, \ldots, N-1,$$

are the eigenvalues associated with the FST on the interval $[y_{\mathrm{L}}, y_{\mathrm{R}}]$. The $N-1$ functions $\widehat{V_{x,l'}}$ are decoupled completely. Since $u_{x,l}^n$, thus $|u_{x,l'}^n|^2$, is supported in $[x_{\mathrm{LP}}, x_{\mathrm{RP}}]$, Eq. (6.13) is equivalent to

$$-\partial_x^2 \widehat{V_{x,l'}} + \lambda_{l'} \widehat{V_{x,l'}} = \widehat{|u_{x,l'}^n|^2}, \quad x \in [x_{\mathrm{LP}}, x_{\mathrm{RP}}], \quad l' = 1, \ldots, N-1, \tag{6.14}$$

$$-\partial_x \widehat{V_{x,l'}}(x_{\mathrm{LP}}) = -\sqrt{\lambda_{l'}} \widehat{V_{x,l'}}(x_{\mathrm{LP}}), \tag{6.15}$$

$$\partial_x \widehat{V_{x,l'}}(x_{\mathrm{RP}}) = -\sqrt{\lambda_{l'}} \widehat{V_{x,l'}}(x_{\mathrm{RP}}), \quad l' = 1, \ldots, N-1. \tag{6.16}$$

After $V_{x,l}$ is computed, $u^*_{x,l}$ is then computed through Eq. (6.9) as

$$u^*_{x,l} = u^n_{x,l} e^{-iV_{x,l}\Delta t}.$$

As to Eq. (6.11), by the FST it is equivalent to

$$i\partial_t \widehat{u_{x,l'}} + c\partial_x(c\partial_x \widehat{u_{x,l'}}) - \lambda_{l'}\widehat{u_{x,l'}} = 0, \quad x \in [x_{LP}, x_{RP}], \quad l' = 1, \ldots, N-1.$$

This expresses a set of $N-1$ decoupled PDEs.

Combining the Strang's splitting technique, we can obtain a second-order scheme

Step 0: Given $u^n_{x,l}$;

Step 1: Compute $V_{x,l}$ through

$$-\partial_x^2 \widehat{V_{x,l'}} + \lambda_{l'}\widehat{V_{x,l'}} = \widehat{|u^n_{x,l'}|^2}, \quad x \in [x_{LP}, x_{RP}], \quad l' = 1, \ldots, N-1, \tag{6.17}$$

$$-\partial_x \widehat{V_{x,l'}}(x_{LP}) = -\sqrt{\lambda_{l'}}\widehat{V_{x,l'}}(x_{LP}), \tag{6.18}$$

$$\partial_x \widehat{V_{x,l'}}(x_{RP}) = -\sqrt{\lambda_{l'}}\widehat{V_{x,l'}}(x_{RP}), \quad l' = 1, \ldots, N-1; \tag{6.19}$$

Step 2: Set

$$u^*_{x,l} = u^n_{x,l} e^{-iV_{x,l}\Delta t/2};$$

Step 3: Solve the following equation with the initial datum $u^*_{x,l}$ in $[t_n, t_{n+1}]$, to obtain $u^{**}_{x,l}$

$$i\partial_t \widehat{u_{x,l'}} + c\partial_x(c\partial_x \widehat{u_{x,l'}}) - \lambda_{l'}\widehat{u_{x,l'}} = 0, \quad x \in [x_{LP}, x_{RP}], \quad l' = 1, \ldots, N-1; \tag{6.20}$$

Step 4: Compute $V_{x,l}$ through

$$-\partial_x^2 \widehat{V_{x,l'}} + \lambda_{l'}\widehat{V_{x,l'}} = \widehat{|u^{**}_{x,l'}|^2}, \quad x \in [x_{LP}, x_{RP}], \quad l' = 1, \ldots, N-1, \tag{6.21}$$

$$-\partial_x \widehat{V_{x,l'}}(x_{LP}) = -\sqrt{\lambda_{l'}}\widehat{V_{x,l'}}(x_{LP}), \tag{6.22}$$

$$\partial_x \widehat{V_{x,l'}}(x_{RP}) = -\sqrt{\lambda_{l'}}\widehat{V_{x,l'}}(x_{RP}), \quad l' = 1, \ldots, N-1; \tag{6.23}$$

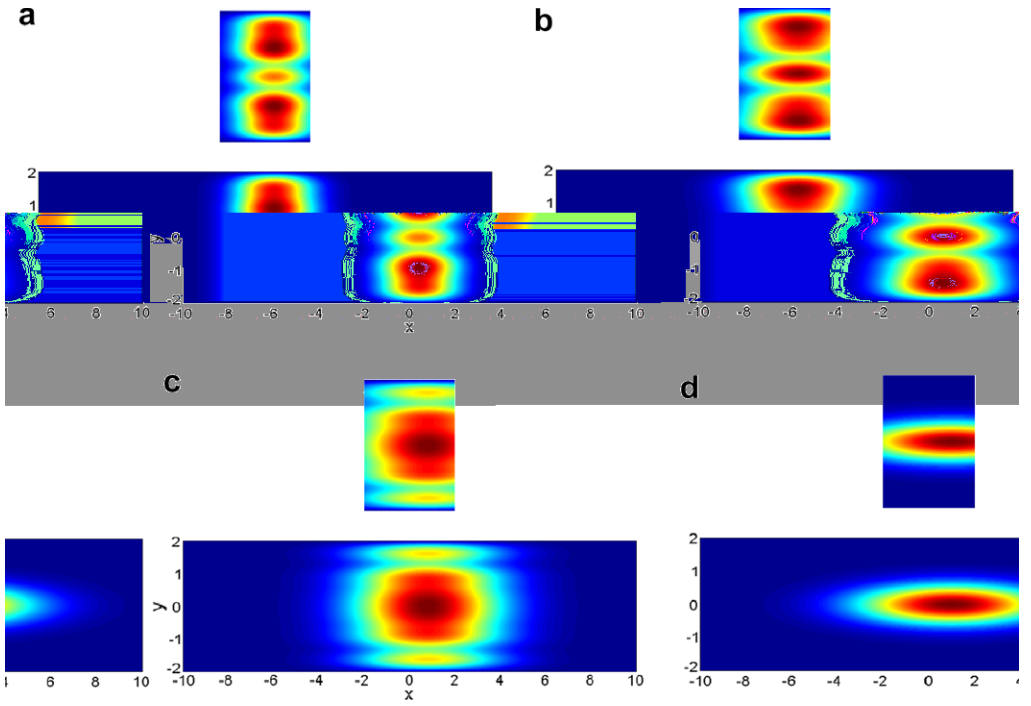

Fig. 13. Snapshots of numerical solutions for the Schrödinger–Poisson system. Top: numerical solution. Bottom: reference solution. (a) $t = 0.2$; (b) $t = 0.3$; (c) $t = 0.4$; (d) $t = 0.5$.

Step 5: Set

$$u_{x,l}^{n+1} = u_{x,l}^{**} e^{-iV_{x,l}\Delta t/2}.$$

The discretization in the x direction is achieved with the central difference scheme, and the time derivative in Eq. (6.20) is approximated by the Crank–Nicolson scheme. All the resulting linear systems have tridiagonal coefficient matrices, thus are easy to solve. We omit the detailed discussion here. We would remark that other types of physical boundary conditions can be considered analogously.

Now we use our scheme to study the evolution of a traveling Gaussian beam in a waveguide of width 4. The initial function is

$$u_0(x) = e^{-4x^2-4y^2+ix},$$

which is well supported in $[-2, 2]^2$. We set the computational domain as $[-3, 3]\times[-2, 2]$, and let $\sigma_0 = 10$. The numerical solution is obtained with $h_x = h_y = 0.01$, $\Delta t = 0.001$. To make comparison, we have both the spatial stepsize and the time step, and perform the computation on a large computational domain $[-11, 11]\times[-2, 2]$ to get a reference solution. Fig. 13 shows both the numerical solution and the reference solution at different time points. We see that they match very well.

7. Conclusions

The PML absorbing boundary conditions have been widely used to simulate waves in unbounded domains. The fundamental idea, which is best interpreted as a complex continuation of the real variable, has been extended to much complicated fluid dynamics problems.

In this paper, we have applied the PML technique to the nonlinear Schrödinger wave equations. The success lies in the time-transverse invariant property which holds for both the original and the PML-modified Schrödinger wave equations. It has been shown by numerical experiments that if waves keep moving out of the physical domain, the PML method usually presents good numerical approximations, no matter which kind of Schrödinger wave equation (with real potential) is considered. Of great interest is the PML for the Schrödinger–coupled systems. Though only a simple-versioned Schrödinger–Poisson system has been considered in this paper, its generalization to more complicated versions, such as the N-particle Schrödinger–Poisson system and the Schrödinger–Poisson-Xα model, and other coupled systems, such as Schrödinger-Maxwell system, is straightforward.

Our numerical tests have revealed that though the PML absorbing layers can be made perfectly absorbing for the linear Schrödinger equation with constant potentials, this is not possible for other Schrödinger wave equations. Intrinsic reflection appears in the PML absorbing layers. How to further improve the performance of PML is an interesting issue which deserves consideration.

Acknowledgments

Supported partially by the National Natural Science Foundation of China under Grant No. 10401020, the Alexander von Humboldt Foundation, and the Key Project of China High Performance Scientific Computation Research.

References

[1] N.B. Abdallah, F. Méhats, On a Vlasov–Schrödinger–Poisson model, Comm. Partial Differential Equations 29 (2004) 173–206.
[2] I. Alonso-Mallo, N. Reguera, Discrete absorbing boundary conditions for Schrödinger-type equations, Practical Implementation Math. Comp. 73 (245) (2003) 127–142.
[3] X. Antoine, C. Besse, Unconditionally stable discretization schemes of non-reflecting boundary conditions for the one-dimensional Schrödinger equation, J. Comput. Phys. 181 (1) (2003) 157–175.
[4] X. Antoine, C. Besse, S. Descombes, Artificial boundary conditions for one-dimensional cubic nonlinear Schrödinger equations, SIAM J. Numer. Anal. 43 (6) (2006) 2272–2293.
[5] X. Antoine, C. Besse, V. Mouysset, Numerical schemes for the simulation of the two-dimensional Schrödinger equation using non-reflecting boundary conditions, Math. Comp. 248 (2004) 1779–1799.

[6] D. Appelö, T. Hagstrom, G. Kreiss, Perfectly matched layers for hyperbolic systems: general formulation, well-posedness, and stability, SIAM J. Appl. Math. 67 (1) (2006) 1–23.
[7] A. Arnold, Self-consistent relaxation-time models in quantum mechanics, Comm. PDE 21 (1996) 473–506.
[8] A. Arnold, M. Ehrhardt, Discrete transparent boundary conditions for wide angle parabolic equations in underwater acoustics, J. Comput. Phys. 145 (1998) 611–638.
[9] A. Arnold, M. Ehrhardt, I. Sofronov, Discrete transparent boundary conditions for the Schrödinger equation: fast calculation, approximation, and stability, Comm. Math. Sci. 1 (3) (2003) 501–556.
[10] E. Bécache, P.G. Petropoulos, S.D. Gedney, On the long-time behaviour of unsplit perfectly matched layers, IEEE Trans. Antennas Propagat. 52 (5) (2004) 1335–1342.
[11] W. Bao, S. Jin, P.A. Markowich, On time-splitting spectral approximations for the Schrödinger equation in the semiclassical regime, J. Comput. Phys. 175 (2002) 487–524.
[12] W. Bao, Shi Jin, P.A. Markowich, Numerical study of time-Splitting spectral discretizations of nonlinear Schrödinger equations in the semi-classical regimes, SIAM J. Sci. Comp. 25 (2003) 27–64 (Electronic).
[13] V.A. Baskakov, A.V. Popov, Implementation of transparent boundaries for the numerical solution of the Schrödinger equation, Wave Motion 14 (1991) 123–128.
[14] J.P. Bérenger, A perfectly matched layer for the absorption of electromagnetic waves, J. Comput. Phys. 114 (1994) 185–200.
[15] A. Bermúdez, L. Hervella-Nieto, A. Prieto, R. Rodrǵuez, An exact bounded PML for the Helmholtz equation, C.R. Acad. Sci. Paris. Serie I 339 (2004) 803–808.
[16] W. Chew, W. Weedon, A 3D perfectly matched medium from modified Maxwell's equations with stretched coordinates, Microwave Optical Technol. Lett. 7 (1994) 599–604.
[17] F. Collino, Perfectly matched absorbing layers for the paraxial equations, J. Comp. Phys 131 (1997) 164–180.
[18] F. Collino, P. Monk, The perfectly matched layer in curvilinear coordinates, SIAM J. Sci. Comput. 19 (1998) 2061–2090.
[19] A.S. Davydov, Solitons in molecular systems, Physica Scripta 20 (1979) 387–394.
[20] P. Deuflhard, F. Schmidt, Discrete transparent boundary conditions for the numerical solution of Fresnel's equation, Comput. Math. Appl. 29 (9) (1995) 53–76.
[21] T. Fevens, H. Jiang, Absorbing boundary conditions for the Schrödinger equation, SIAM J. Sci. Comput. 21 (1999) 255–282.
[22] T. Friese, F. Schmidt, D. Yevick, A comparison of transparent boundary conditions for the Fresnel equation, J. Comput. Phys. 168 (2001) 433–444.
[23] A.S. Fokas, The generalized Dirichlet-to-Neumann map for certain nonlinear evolution PDEs, Comm. Pure Appl. Math. 58 (5) (2005) 639–670.
[24] D. Givoli, Numerical Methods for Problems in Infinite Domains, Elsevier, Amsterdam, 1992.
[25] D. Givoli, High-order local non-reflecting boundary conditions: a review, Wave Motion 39 (2004) 319–326.
[26] M.N. Guddati, K.W. Lim, Continued fraction absorbing boundary conditions for convex polygonal domains, Inter. J. Numer. Methods Eng. 66 (2006) 949–977.
[27] T. Hagstrom, Radiation boundary conditions for the numerical simulation of waves, Acta Numer 8 (1999) 47–106.
[28] T. Hagstrom, New results on absorbing layers and radiation boundary conditions, in: M. Ainsworth et al. (Eds.), Topics in Computational Wave Propagation, Springer-Verlag, 2003, pp. 1–42.
[29] H.D. Han, Z.Y. Huang, Exact artificial boundary conditions for Schrödinger equation in R^2, Comm. Math. Sci. 2 (1) (2004) 79–94.
[30] H.D. Han, X.N. Wu, Z.L. Xu, Artificial boundary method for Burgers' equation using nonlinear boundary conditions, J. Comput. Math. 24 (3) (2006) 295–304.
[31] J.R. Hellums, W.R. Frensley, Non-Markovian open-system boundary conditions for the time-dependent Schrödinger equation, Phys. Rev. B 49 (1994) 2904–2906.
[32] R. Higdon, Absorbing boundary conditions for difference approximations to the multidimensional wave equation, Math. Comp. 47 (1986) 437–459.
[33] R. Higdon, Numerical absorbing boundary conditions for the wave equation, Math. Comp. 49 (1987) 65–90.
[34] F.Q. Hu, On the construction of PML absorbing boundary condition for the nonlinear Euler equations, AIAA paper 2006-0798 (2006).
[35] S. Jiang, L. Greengard, Fast evaluation of non-reflecting boundary conditions for the Schrödinger equation in one dimension, Comput. Math. Appl. 47 (2004) 955–966.
[36] H.L. Li, C.K. Lin, Semiclassical limit and well-posedness of nonlinear Schrodinger–Poisson, Electronic J. Diff. Eqs. 93 (2003) 1–17.
[37] C. Lubich, A. Schädle, Fast convolution for non-reflecting boundary conditions, SIAM J. Sci. Comput. 24 (2002) 161–182.
[38] P.A. Markowich, C. Ringhofer, C. Schmeiser, Semi-Conductor Equations, Spring-Verlag, Wien, NY, 1990.
[39] B. Mayfield, Non Local Boundary Conditions for the Schrödinger Equation, Ph.D. Thesis, University of Rhodes Island, Providence, RI, 1989.
[40] J.S. Papadakis, Impedance formulation of the bottom boundary condition for the parabolic equation model in underwater acoustics, NORDA Parabolic Equation Workshop, NORDA Tech. Note 143 (1982).
[41] P. Petropoulos, Reflectionless sponge layers as absorbing boundary conditions for the numerical solution of Maxwell's equations in rectangular, cylindrical and spherical coordinates, SIAM J. Appl. Math. 60 (2000) 1037–1058.
[42] D. Pathria, J.L. Morris, Pseudo-spectral solution of nonlinear Schrödinger equations, J. Comput. Phys. 87 (1990) 108–125.
[43] V.M. Pérez-García, X.Y. Liu, Numerical methods for the simulation of trapped nonlinear Schrödinger systems, Appl. Math. Comp. 144 (2003) 215–235.
[44] A. Schädle, Non-reflecting boundary conditions for the two-dimensional Schrödinger equation, Wave Motion 35 (2) (2002) 181–188.

[45] F. Schmidt, D. Yevick, Discrete transparent boundary conditions for Schrödinger-type equations, J. Comput. Phys. 134 (1997) 96–107.
[46] A. Soffer, C. Stucchio, Open boundaries for the nonlinear Schrödinger equation, J. Comput. Phys. 225 (2) (2007) 1218–1232.
[47] G. Strang, On the construction and comparison of difference schemes, SIAM J. Numer. Anal. 5 (3) (1968) 506–517.
[48] Z.Z. Sun, X.N. Wu, The stability and convergence of a difference scheme for the Schrödinger equation on an infinite domain by using artificial boundary conditions, J. Comp. Phys. 214 (1) (2006) 209–223.
[49] J. Szeftel, Absorbing boundary conditions for one-dimensional nonlinear Schrödinger equations, Numer. Math. 104 (2006) 103–127.
[50] J. Szeftel, Design of absorbing boundary conditions for Schrödinger equations in R^d, SIAM J. Numer. Anal. 42 (4) (2004) 1527–1551.
[51] S.V. Tsynkov, Numerical solution of problems on unbounded domains: a review, Appl. Numer. Math. 27 (1998) 465–532.
[52] J.A.C. Weideman, B.M. Herbst, Split-step methods for the solution of the nonlinear Schrödinger equation, SIAM J. Numer. Anal. 23 (3) (1986) 485–507.
[53] Z.L. Xu, H.D. Han, X.N. Wu, Numerical method for the deterministic Kardar–Parisi–Zhang equation in unbounded domains, Comm. Comput. Phys. 1 (2006) 479–493.
[54] C.X. Zheng, Exact non-reflecting boundary conditions for one-dimensional cubic nonlinear Schrödinger equations, J. Comput. Phys. 215 (2) (2006) 552–565.